

This is the accepted manuscript made available via CHORUS. The article has been published as:

Direct Measurement of the Astrophysical $F_{19}^{\alpha\gamma}$ Reaction in the Deepest Operational Underground Laboratory

L. Y. Zhang et al.

Phys. Rev. Lett. **127**, 152702 — Published 7 October 2021

DOI: [10.1103/PhysRevLett.127.152702](https://doi.org/10.1103/PhysRevLett.127.152702)

Direct measurement of astrophysical $^{19}\text{F}(p, \alpha)^{16}\text{O}$ reaction in the deepest operational underground laboratory

L.Y. Zhang¹, J. Su¹, J.J. He^{1,*}, M. Wiescher^{2,†}, R.J. deBoer², D. Kahl³, Y.J. Chen¹, X.Y. Li¹, J.G. Wang⁴, L. Zhang⁵, F.Q. Cao⁵, H. Zhang⁵, Z.C. Zhang⁷, T.Y. Jiao⁴, Y.D. Sheng¹, L.H. Wang¹, L.Y. Song¹, X.Z. Jiang¹, Z.M. Li¹, E.T. Li⁷, S. Wang⁸, G. Lian⁵, Z.H. Li⁵, X.D. Tang⁴, H.W. Zhao⁴, L.T. Sun⁴, Q. Wu⁴, J.Q. Li⁴, B.Q. Cui⁵, L.H. Chen⁵, R.G. Ma⁵, B. Guo⁵, N.C. Qi⁹, W.L. Sun⁹, X.Y. Guo⁹, P. Zhang⁹, Y.H. Chen⁹, Y. Zhou⁹, J.F. Zhou⁹, J.R. He⁹, C.S. Shang⁹, M.C. Li⁹, X.H. Zhou⁴, H.S. Xu⁴, J.P. Chen¹, and W.P. Liu^{5‡}

¹Key Laboratory of Beam Technology and Material Modification of Ministry of Education, College of Nuclear Science and Technology, Beijing Normal University, Beijing 100875, China

²The Joint Institute for Nuclear Astrophysics, Department of Physics, University of Notre Dame, Notre Dame, Indiana 46556 USA

³Extreme Light Infrastructure – Nuclear Physics, Horia Hulubei National Institute for R&D in Physics and Nuclear Engineering (IFIN-HH), Bucharest-Măgurele 077125, Romania

⁴Institute of Modern Physics, Chinese Academy of Sciences, Lanzhou 730000, China

⁵China Institute of Atomic Energy, Beijing 102413, China

⁷College of Physics and Optoelectronic Engineering, Shenzhen University, Shenzhen 518060, China

⁸Shandong Provincial Key Laboratory of Optical Astronomy and Solar-Terrestrial Environment, Institute of Space Sciences, Shandong University, Weihai 264209, China and

⁹Yalong River Hydropower Development Company, Chengdu 610051, China

(Dated: August 25, 2021)

Fluorine is one of the most interesting elements in nuclear astrophysics, where the $^{19}\text{F}(p, \alpha)^{16}\text{O}$ reaction is of crucial importance for Galactic ^{19}F abundances and CNO cycle loss in first generation Pop III stars. As a day-one campaign at the Jinping Underground Nuclear Astrophysics experimental facility (JUNA), we report direct measurements of the essential $^{19}\text{F}(p, \alpha)^{16}\text{O}$ reaction channel. The γ -ray yields were measured over $E_{\text{c.m.}} = 72.4\text{--}344$ keV, covering the Gamow window; our energy of 72.4 keV is unprecedentedly low, reported here for the first time. The experiment was performed under the extremely low cosmic-ray-induced background environment of the China JinPing underground Laboratory (CJPL), one of the deepest underground laboratories in the world. The present low-energy S -factors deviate significantly from previous theoretical predictions, and the uncertainties are significantly reduced. The thermonuclear $^{19}\text{F}(p, \alpha)^{16}\text{O}$ reaction rate has been determined directly at the relevant astrophysical energies.

The astrophysical origin of fluorine is puzzling. Fluorine is a monoisotopic element, and the stable nuclide ^{19}F is rather fragile – a curious and critically important point in nuclear astrophysics. It does not contribute to, nor is it synthesized in, the main nuclear reactions taking place in stars. ^{19}F has a limited number of atomic and molecular absorption lines in stellar spectra from which reliable abundances are derived, making the nucleosynthetic origin of ^{19}F the least understood of all the light elements [1]. In stellar interiors, ^{19}F is readily annihilated by the most abundant elements, hydrogen and helium, via the $^{19}\text{F}(p, \alpha)^{16}\text{O}$ and $^{19}\text{F}(\alpha, p)^{22}\text{Ne}$ reactions, respectively. In order to explain the presence of fluorine, a mechanism is required that enables it to escape from the hot stellar interior after it forms.

Theoretical calculations and observational data suggest several possible ^{19}F production sites [2, 3]. Woosley and Haxton [4] calculated ^{19}F production in Type II core-collapse supernovae (SNe) by neutrino spallation on ^{20}Ne ; Jorissen *et al.* [5] observed the ^{19}F overabundances (with respect to solar) in red giant stars and provided evidence for ^{19}F production during shell He burning in asymptotic giant branch (AGB) stars [6, 7]; Meynet and

Arnould [8] identified He burning in Wolf-Rayet stars. Kobayashi *et al.* [9] considered the neutrino-process nucleosynthesis as the major origin of ^{19}F in metal-deficient stars (Type II and Ia supernovae and hypernovae) as well as AGB stars, and such supernova provides a celestial site to study the neutrino-nucleus interactions and flavor oscillations in high density matter [10]. In addition, a signature of fluorine was indeed observed in the spectra of Nova Mon 2012 [11]; however, classical novae seem to account for $\leq 1\%$ of its solar abundance [12]. Therefore, it remains an open question, to what extent each candidate site may contribute to the solar-system and Galactic fluorine, and a precise rate of the $^{19}\text{F}(p, \alpha)^{16}\text{O}$ reaction plays an essential role.

One of the major contributors to Galactic fluorine production is thought to be AGB stars [5]. Yet, the astrophysically observed fluorine overabundances cannot be understood using current AGB models, and it seems that additional mixing effects should be involved, i.e., fluorine is produced in the He-rich intershell and carried to the surface via recurrent dredge-up episodes [13]. Palmerini *et al.* [14] analyzed the possible effect of such extra mixing within an AGB star, and investigated the impact of

different rates of the $^{19}\text{F}(p, \alpha)^{16}\text{O}$ destruction reaction. They found that the surface abundance of ^{19}F varied by up to 50% when changing the rate of this reaction by a factor of ≈ 2 .

Furthermore, the possibility of a break-out from the cold CNO cycles [15], which is the leakage out of the CNO cycle towards the NeNa cycle via the $^{19}\text{F}(p, \gamma)^{20}\text{Ne}$ reaction, not only depends on the abundance of ^{19}F but also on the reaction rates of the $^{19}\text{F}(p, \gamma)^{20}\text{Ne}$ breakout reaction and the competing $^{19}\text{F}(p, \alpha)^{16}\text{O}$ back-processing reaction. The enhancement of this $(p, \gamma)/(p, \alpha)$ rate ratio by a factor of 8 or more could possibly solve the Ca production problem, and support the faint supernova model, and thus ultimately determine evolution destiny for the first generation Pop III stars (e.g., Keller star [16]) [17]. Therefore, experimental characterization of these reaction rates in the low temperature region (~ 0.1 GK) are strongly desired to meet the requirements of astrophysical models.

The $^{19}\text{F}(p, \alpha)^{16}\text{O}$ reaction occurs via three types of channels, i.e., (p, α_0) , (p, α_π) and (p, α_γ) [18]. The (p, α_π) channel provides less than $\approx 10\%$ contribution at low temperatures ≈ 0.05 GK [19, 20]; the (p, α_γ) channel dominates at temperatures above 0.2 GK, while the (p, α_0) channel dominates at the lower temperatures below ≈ 0.15 GK [19, 21]. However, recent studies have shown that the (p, α_γ) channel could possibly dominate the total rate even below ≈ 0.05 GK [18, 22], where a significantly enhanced reaction rate is possible, owing to the interference between a possible 11-keV resonance and the well-known 323-keV resonance. Such theoretical prediction and extrapolation require a new measurement. So far, in the low temperature region, below ≈ 0.2 GK, the thermonuclear $^{19}\text{F}(p, \alpha)^{16}\text{O}$ reaction rate is still not known precisely enough to address the fluorine abundance as well as CNO material loss. The Gamow energy window of present astrophysical interest is located between $E_{c.m.} \approx 70\text{--}350$ keV (in center-of-mass frame). Currently, the (p, α_γ) and (p, α_0) channels were measured at above-ground laboratories down to $E_{c.m.} \approx 189$ keV [23] and 172 keV [24], respectively. In the low energy region, e.g., at ≈ 70 keV, the extrapolated cross sections have uncertainties of up to five orders of magnitude [23–25]. The rate of cosmic-ray background radiation makes lower-energy direct measurements in laboratories at the Earth's surface (i.e., the above-ground lab) very challenging.

The China Jinping underground laboratory (CJPL) is located in a traffic tunnel under Jinping Mountain, southwest of China [26] with about 2400-m rock overburden vertically. It is the deepest operational underground laboratory for particle and nuclear physics experiments in the world. In this underground environment, the muon and neutron fluxes are reduced by 6 and 4 orders of magnitude, respectively, compared to those at the Earth's surface. Owing to the depth, the cosmic-ray

induced background measured at CJPL [27] is significantly lower than that in LUNA (1400-m-thick dolomite rocks) [28]. With such a unique super-low-background environment [29], the Jinping Underground Nuclear Astrophysics experimental facility (JUNA) [30] was initiated in 2015. One of the subprojects [25] is dedicated to directly measuring the $^{19}\text{F}(p, \alpha_\gamma)^{16}\text{O}$ reaction at Gamow energies.

In this Letter, we report on the results of a direct measurement of the $^{19}\text{F}(p, \alpha_\gamma)^{16}\text{O}$ reaction at JUNA. The astrophysical S factors have been derived in the energy region of $E_{c.m.} \approx (72.4\text{--}188.8)$ keV. We report the lowest energy measurements, extending down to 72.4 keV, directly cover the Gamow window. Our measurement decreases the uncertainty presented in previous S factor extrapolations [22, 23] from orders of magnitude to the 10% level, which sets a solid experimental basis for astrophysical modeling.

The experiment was carried out on the high-current 400 kV JUNA accelerator [31] at CJPL. The experimental setup is shown in the Supplemental Material [32], which is similar to the one described in Ref. [33]. A proton beam from the accelerator was undulated over a rectangular area of about 4×4 cm² by oscillating the magnetic field of the beam deflector. In this way, a well-focused intense beam was distributed uniformly, and thus target damage was reduced. The scanning proton beam was collimated by two $\phi(10\text{--}20)$ mm apertures and then impinged on a water-cooled target, where the beam current reached up to 1 mA, with a spot size of about $\phi 10$ mm. Two very strong and durable implanted ^{19}F targets, developed in recent years [33, 34], were utilized in this work. A 4π BGO detector array specially designed for the JUNA project [35] was equipped to detect the γ -rays, which was already characterized in previous work (e.g., see Ref. [33]). The full details of the experiment will be described in a forthcoming paper [36].

Figure 1 shows the normalized γ -ray spectra taken at a proton beam energy of $E_p = 130$ keV with the 4π BGO array. Here, E_p denotes the proton beam energy before the Cr protective layer of the implanted fluorine target, and the bombarding energy on the fluorine atoms is corrected for the energy loss through the Cr layer with a Geant4 simulation [37]. The above-ground (taken at CIAE) and underground (taken at JUNA) spectra are shown for comparison. In the above-ground experiment, the BGO array was covered by a plastic scintillator to suppress the cosmic-ray background (as a μVeto signal). In addition, we observed the γ rays induced by the ^{12}C and ^{13}C impurities from the target, as well as those induced by the ^{11}B contaminant mainly from the beam apertures, and their origins were analyzed in Ref. [33]. This simple comparison clearly shows the advantage of the deep underground measurement owing to the extremely low environmental background.

Figure 2 shows typical γ -ray spectra taken at three

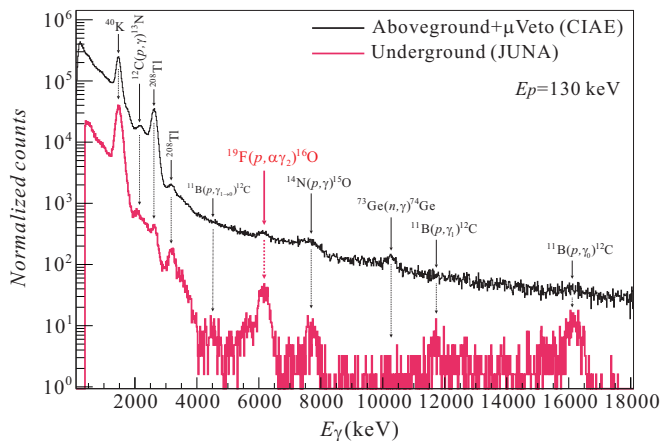


FIG. 1. γ -ray spectra of the $^{19}\text{F}+p$ experiments measured by a 4π BGO array at a proton energy of $E_p = 130$ keV. The above-ground (at CIAE) and underground (at JUNA) spectra are shown for comparison. Two background lines at 1460.8 keV (from ^{40}Ar) and 2614.5 keV (from ^{208}Tl) are used for energy calibration. The γ rays induced by the ^{12}C , ^{13}C and ^{11}B contaminants are also indicated.

proton beam energies. It shows that the 6917-keV (from α_3 channel) and 7117-keV (from α_4 channel) γ rays were also observed at certain proton energies, compared to the dominant 6130-keV γ rays, their total contribution makes a maximum contribution of $\approx 2.4\%$ in the energy region studied in this work. Relying on the deep underground environment, we can now access an energy point down to $E_p = 88$ keV (i.e., $E_{c.m.} \approx 72.4$ keV), where the γ rays induced by the ^2H contaminant began to move into the 6130-keV region of interest and became the limiting background contribution. An experimental run with a pure Fe target (covered by a 50-nm thick Cr layer) was done at this $E_p = 88$ keV point to evaluate the background contribution from our implanted fluorine targets (covered also by a 50-nm thick Cr layer) [33], and the normalized spectrum (blue-shaded) is also shown in Fig. 2(c) for comparison. Owing to the possible ^2H contamination, a net count of 30 ± 26 was obtained at this energy under the conditions of ≈ 1.0 mA average beam intensity and ≈ 2 -days machine time (a beam exposure of ≈ 190 C), as shown in the inset. Therefore, the energy of $E_{c.m.} \approx 72.4$ keV can be regarded as a ‘lower-limit’ accessible with current JUNA conditions. Similar to the previous target tests [33, 34], the ^{19}F target material loss was monitored by observing the yield of 6130-keV γ rays at the $E_{c.m.} = 323$ keV resonance during the experiment runs. It was found that the target loss was less than 7% under a total beam exposure of ≈ 270 C. This effect has been corrected by utilizing the relationship between beam exposure and target material loss [36].

Figure 3 shows the experimental yields for the $^{19}\text{F}(p, \alpha\gamma)^{16}\text{O}$ reaction measured at JUNA. The data for two targets (Target#1 and Target#2) are shown sepa-

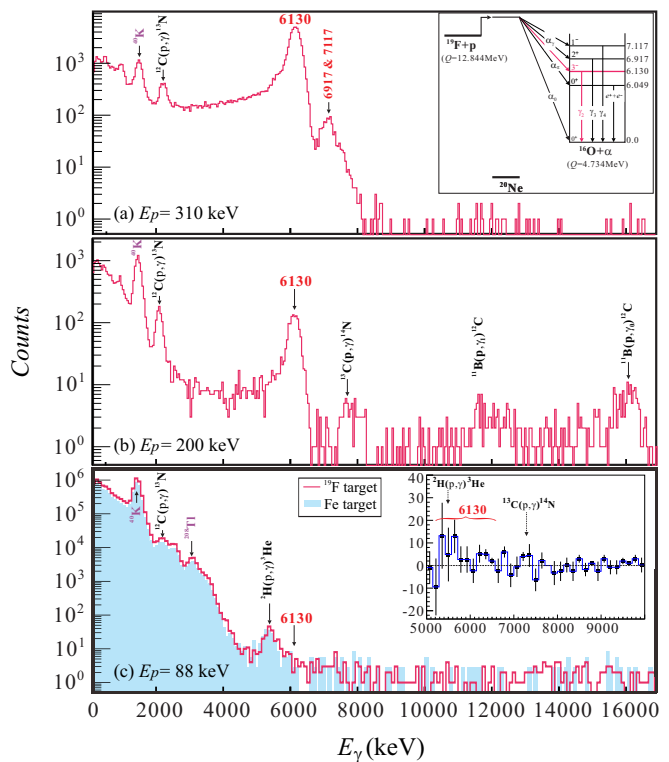


FIG. 2. Typical γ -ray spectra of the $^{19}\text{F}(p, \alpha\gamma)^{16}\text{O}$ reaction measured at JUNA with a 4π BGO array: (a) at $E_p = 310$ keV, (b) at $E_p = 200$ keV, (c) at $E_p = 88$ keV, respectively. For panel (a), the inset shows the reaction scheme [18]; for panel (c), the inset shows the rebinned net spectrum after subtracting the normalized background contribution (blue-shaded), which was evaluated by a pure Fe target (covered also with a 50-nm Cr layer) run. Here, the γ -peak positions for the possible contaminant reactions from ^2H and ^{13}C are indicated by the arrows and integral region for the 6130-keV γ -ray by the curly bracket.

rately. Here, the uncertainties shown are the statistical ones (smaller than 2% for most data, while 87% for the lowest point). We have simulated these data under the Geant4 framework based on full R -matrix calculations, and the two curves shown represent the results simulated by using the ‘best’ R -matrix fit to the S -factor data as discussed below.

Owing to the complicated target structure and the unknown self-sputtering rate during the implantation procedure, the absolute ^{19}F number density is hard to determine precisely. Therefore, we have made a relative measurement of the astrophysical S -factors for the reaction studied. The astrophysical S -factor is more convenient than the cross section, because the Coulomb penetrability is factored out, and a plot flattens relative to the Sommerfeld parameter ($\eta = Z_1 Z_2 e^2 / \hbar v$) [38]. Here, the parameters of ^{19}F depth distribution and the Cr foil thickness were determined by adjusting their values in the Geant4 simulation to reproduce the experimental yield

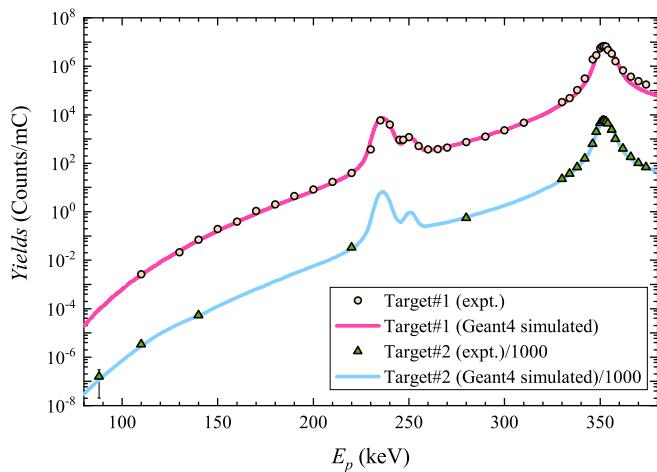


FIG. 3. Experimental yields for the $^{19}\text{F}(p, \alpha\gamma)^{16}\text{O}$ reaction measured by the JUNA experiment (with statistical uncertainties only). The results for two implanted targets are shown separately, where the Target#2 data are scaled down by a factor of 1000. The Geant4 simulated curve is indicated by the solid line for each target, by using the R -matrix calculated S -factor as shown in “fit1” in Fig. 4.

around the 323-keV region. Thus, the product of absolute detection efficiency and ^{19}F number density was determined based on the well-known NACRE [39] strength $\omega\gamma_{(p,\alpha\gamma)} = (23.1 \pm 0.9)$ eV (with an uncertainty of 3.9%) of the 323-keV resonance, which can be regarded as a normalizing factor. With these parameters, the effective beam energies and S -factors for those off-resonance points were determined by the Geant4 simulations as shown in Fig. 4. For the energy points near/on the resonance peaks, the corresponding S -factors were not constant over each energy point and thus are not shown in the plot. It was found that the corresponding experimental yields can be reproduced well by using known strengths of the three resonances at $E_{\text{c.m.}} = 212, 225, 323$ keV, which verifies the present experimental method and analysis procedure. Numeric samples of the S factors and the associated uncertainties in the off-resonance region are tabulated in the Supplemental Material [32].

An R -matrix analysis, using the code AZURE2 [40, 41], was used to fit the off-resonance data. Following Brune [42], the partial widths of the narrow resonances were fixed to those determined from the thick-target yield Geant4 simulations described above. The R -matrix analysis is an extension of that presented in deBoer *et al.* [22], and includes the data considered in that work in addition to the $^{19}\text{F}(p, \alpha_2)^{16}\text{O}$ measurements presented here. Many R -matrix fits were attempted, with the three most probable ones shown in Fig. 4. Here, “Sub” denotes the 1^+ subthreshold state at $E_x = 12.396$ MeV, “11 keV” the 11-keV 1^+ level at $E_x = 12.855$ MeV, and “ 2^+ ” the underlying α -cluster 2^+ state at $E_x = 13.095$ MeV. For

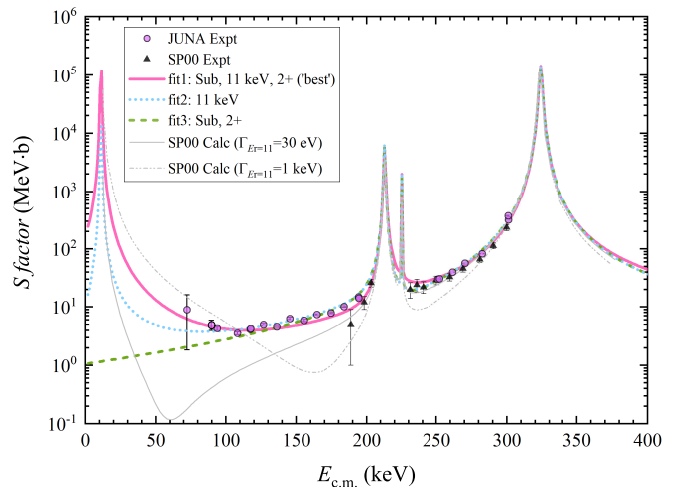


FIG. 4. Astrophysical S factors of the $^{19}\text{F}(p, \alpha\gamma)^{16}\text{O}$ reaction derived from the JUNA experiment (with statistical uncertainties only). The previous experimental data (“SP00 Expt”) [23] and theoretical predictions (“SP00 Calc”) [22, 23] are shown for comparison. Here we show the exact $S(E)$ without taking into account the individual experimental target thicknesses. Three most probable R -matrix fits are shown. See text for details.

example, the label “fit1: Sub, 11 keV, 2^+ (‘best’)” indicates the ‘best’ R -matrix fit, found by considering the subthreshold state, a near threshold 11-keV resonance as well as the 2^+ state. Using a multi-channel monte-carlo (MCMC) analysis, we find the presence of the 11-keV resonance at the 2.6σ level. The inclusion of the subthreshold state and underlying 2^+ state further improves the reproduction of the experimental data. The ‘best fit’ R -matrix parameters are listed in the Supplemental Material [32]. The various extrapolations exhibit quite different trends below the lowest energy point achieved, but the JUNA experimental data now extend directly into the Gamow energy range, significantly reducing the uncertainty in the S -factor over the range of astrophysical interest compared estimates based on previous data as detailed in deBoer *et al.* [22] and Zhang *et al.* [18] (see Fig. 4). In addition, the extrapolations from Spyrou *et al.* [23] are also shown for comparison (two grey lines, labelled as SP00).

The thermonuclear $^{19}\text{F}(p, \alpha\gamma)^{16}\text{O}$ reaction rate as a function of temperature has been calculated by numerical integration of the S factors with the well-known formula for $N_A \langle \sigma v \rangle$ in Rolfs and Rodney [38]. In this way, the present mean rate and the associated uncertainties (Low and High limits) are obtained in a temperature region of 0.01–1 GK, which are fully tabulated in the Supplemental Material [32, 43].

The new data constrain the $^{19}\text{F}(p, \alpha\gamma)$ reaction rate for the temperature region down to 0.05 GK, which covers the temperature range of interest for faint supernovae (see, e.g. Clarkson and Herwig [17]). Figure 5 shows

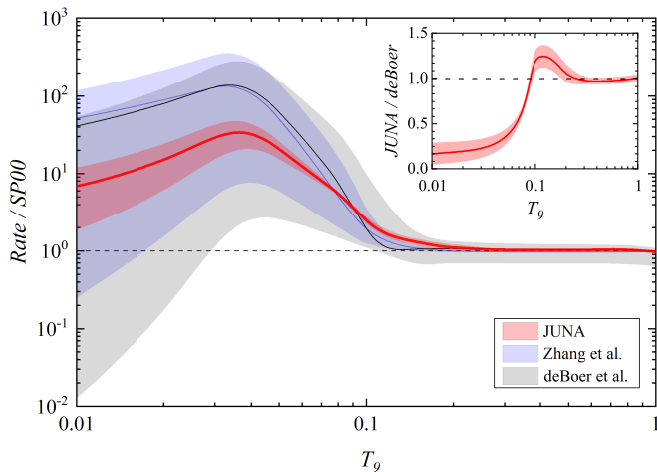


FIG. 5. Ratio of present (labelled as JUNA) relative to Spyrou *et al.*'s rate (labelled as SP00 [23]). The corresponding ratios for deBoer *et al.*'s rate [22] and Zhang *et al.*'s rate [18] are also shown for comparison. The associated uncertainties are shown as the colored bands. The inset shows the ratio between the present and deBoer *et al.*'s rates. For more information, refer to Supplemental Material [32].

the comparison between our JUNA rate and the previous rate of Spyrou *et al.* [23] (labelled as SP00). Our rate is significantly larger than that of Spyrou *et al.* [23] below ≈ 0.2 GK. The comparison is also shown for the recently reevaluated rates by deBoer *et al.* [22] and by Zhang *et al.* [18], where both evaluations gave similar central rates, yet with larger uncertainty estimates based on previous data. Our new JUNA rate deviates significantly from the previous ones by factor of 0.2–1.3 (as shown in the inset). We reported the most precise value for the $^{19}\text{F}(p, \alpha\gamma)$ rate ever achieved.

Together with the previous investigations on the $^{19}\text{F}(p, \alpha_0)^{16}\text{O}$ channel [19, 21, 22, 24], the present work provides strong experimental support that the (p, α_0) channel dominates the total (p, α) rate over the entire low temperature region below ≈ 0.12 GK, and thus clar-

ifies the role of these two channels [18, 22].

In summary, as a day-one campaign at JUNA, we have directly measured the important $^{19}\text{F}(p, \alpha\gamma)^{16}\text{O}$ reaction down to the lowest energy point of $E_{c.m.} \approx 72.4$ keV, relying on the extra-low background deep underground environment in CJPL. This is almost an impossible task in the above-ground lab with traditional techniques. The measurement covered the energy region of $E_{c.m.} \approx (72.4\text{--}344)$ keV, where the experimental data below 188.8 keV were measured (except the earlier unpublished results [44]), for the first time, within the Gamow energy region for this reaction of astrophysical interest. It shows that the present $^{19}\text{F}(p, \alpha\gamma)^{16}\text{O}$ S factors are much larger than the previous predictions, and the associated uncertainties are significantly reduced. The thermonuclear $^{19}\text{F}(p, \alpha\gamma)^{16}\text{O}$ rate has been determined for the temperature region down to 0.05 GK based on direct experimental data, which is now sufficient for the requirements of astrophysics models. The current experiment demonstrated the capability of JUNA, where more deep underground experiments are expected in the future.

Acknowledgments

We wish to thank the staff of the CJPL and Yalong River Hydropower Development Company for logistics support. This work was financially supported by the National Natural Science Foundation of China (Nos. 11490562, 11825504, 12075027, 11961141004). RJD utilized resources from the Notre Dame Center for Research Computing and RJD and MW were supported by the National Science Foundation through Grant No. Phys-2011890, and the Joint Institute for Nuclear Astrophysics through Grant No. PHY-1430152 (JINA Center for the Evolution of the Elements). RJD acknowledges useful discussions with Daniel Odell regarding Bayesian uncertainty estimation applied to R -matrix theory. DK acknowledges the support of the Romanian Ministry of Research and Innovation under research contract 10N/PN 19 06 01 05.

* Corresponding author: hejianjun@bnu.edu.cn

† Corresponding author: Michael.C.Wiescher.1@nd.edu

‡ Corresponding author: wpliu@ciae.ac.cn

- [1] D. Clayton, *Handbook of Isotopes in the Cosmos: Hydrogen to Gallium*, 1st ed. (Cambridge University Press, Cambridge, 2003).
- [2] A. Renda *et al.*, Mon. Not. R. Astron. Soc. **354**, 575 (2004).
- [3] S. Lucatello, T. Masseron, J. A. Johnson, M. Pignatari, and F. Herwig, *Astrophys. J.* **729**, 40 (2011).
- [4] S. E. Woosley and W. C. Haxton, *Nature* **334**, 45 (1988).
- [5] A. Jorissen, V. V. Smith, and D. L. Lambert, *Astron. Astrophys.* **261**, 164 (1992).
- [6] M. Forestini, S. Goriely, A. Jorissen, and M. Arnould, *Astron. Astrophys.* **261**, 157 (1992).
- [7] S. Cristallo *et al.*, *Astrophys. J.* **696**, 797 (2009).
- [8] G. Meynet and M. Arnould, *Astron. Astrophys.* **355**, 176 (2000).
- [9] C. Kobayashi *et al.*, *Astrophys. J. Lett.* **739**, L57 (2011).
- [10] H. Ko *et al.*, *Astrophys. J. Lett.* **891**, L24 (2020).

- [11] S. N. Shore, I. De Gennaro Aquino, G. J. Schwarz, T. Augusteijn, C. C. Cheung, F. M. Walter, and S. Starrfield, *Astron. Astrophys.* **553**, A123 (2013).
- [12] D. Kahl, J. José, and P. J. Woods, *Astron. Astrophys.* 10.1051/0004-6361/202140339 (2021, in press).
- [13] M. Lugaro *et al.*, *Astrophys. J.* **615**, 934 (2004).
- [14] S. Palmerini *et al.*, *J. Phys.: Conf. Ser.* **1308**, 012016 (2019).
- [15] M. Wiescher, J. Görres, and H. Schatz, *J. Phys. G: Nucl. Part. Phys.* **25**, R133 (1999).
- [16] S. C. Keller *et al.*, *Nature* **506**, 463 (2014).
- [17] O. Clarkson and F. Herwig, *Mon. Not. R. Astron. Soc.* **500**, 2685 (2021).
- [18] L. Y. Zhang, A. Y. López, M. Lugaro, J. J. He, and A. I. Karakas, *Astrophys. J.* **913**, 51 (2021).
- [19] I. Indelicato *et al.*, *Astrophys. J.* **845**, 19 (2017).
- [20] I. Lombardo *et al.*, *Phys. Rev. C* **100**, 044307 (2019).
- [21] J. J. He *et al.*, *Chin. Phys. C* **42**, 015001 (2018).
- [22] R. J. deBoer, O. Clarkson, A. J. Couture, J. Görres, F. Herwig, I. Lombardo, P. Scholz, and M. Wiescher, *Phys. Rev. C* **103**, 055815 (2021).
- [23] K. Spyrou *et al.*, *Eur. Phys. J. A* **7**, 79 (2000).
- [24] I. Lombardo *et al.*, *Phys. Lett. B* **748**, 178 (2015).
- [25] J. J. He *et al.*, *Sci. China-Phys. Mech. Astron.* **59**, 652001 (2016).
- [26] K. J. Kang *et al.*, *J. Phys.: Conf. Ser.* **203**, 012028 (2010).
- [27] Y. C. Wu *et al.*, *Chin. Phys. C* **37**, 086001 (2013).
- [28] C. Brogini, D. Bemmerer, A. Guglielmetti, and R. Menegazzo, *Annu. Rev. Nucl. Part. Sci.* **60**, 53 (2010).
- [29] Y. P. Shen *et al.*, *Sci. China-Phys. Mech. Astron.* **60**, 102022 (2017).
- [30] W. P. Liu *et al.*, *Sci. China-Phys. Mech. Astron.* **59**, 642001 (2016).
- [31] Q. Wu *et al.*, *Nucl. Instr. Meth. A* **830**, 214 (2016).
- [32] See Supplemental Material at <http://link.aps.org/supplemental/10.1103/PhysRevLett> for more details of experiment description, R -matrix fit, astrophysical S factor and reaction rate, which includes Refs. [22,33,36,43].
- [33] L. Y. Zhang *et al.*, *Nucl. Instr. Meth. B* **496**, 9 (2021).
- [34] L. Y. Zhang *et al.*, *Nucl. Instr. Meth. B* **438**, 48 (2019).
- [35] J. Su *et al.*, *Nucl. Instr. Meth. A*, **under preparation**.
- [36] L. Y. Zhang *et al.*, *Phys. Rev. C*, **under preparation**.
- [37] S. Agostinelli *et al.*, *Nucl. Instr. Meth. A* **506**, 250 (2003).
- [38] C. E. Rolfs and W. S. Rodney, *Cauldrons in the Cosmos*, 1st ed. (University of Chicago Press, Chicago, 1988).
- [39] C. Angulo *et al.*, *Nucl. Phys. A* **656**, 3 (1999).
- [40] R. E. Azuma, E. Uberseder, E. C. Simpson, C. R. Brune, H. Costantini, R. J. de Boer, J. Görres, M. Heil, P. J. LeBlanc, C. Ugalde, and M. Wiescher, *Phys. Rev. C* **81**, 045805 (2010).
- [41] E. Uberseder and R. J. deBoer, *AZURE2 User Manual* (2015).
- [42] C. R. Brune, *Phys. Rev. C* **66**, 044611 (2002).
- [43] T. Rauscher and F.-K. Thielemann, *Atom. Data Nucl. Data Tables* **75**, 1 (2000).
- [44] H. Lorentz-Wirzba, PhD. thesis, **Univ. Münster (unpublished, 1978)**.